



THE UNIVERSITY
of EDINBURGH



European Research Council
Established by the European Commission

HIGH-ENERGY LOGARITHMIC CORRECTIONS

with the HEJ framework

Emmet Byrne
emmet.byrne@ed.ac.uk

MPI@LHC, Manchester
November 2023

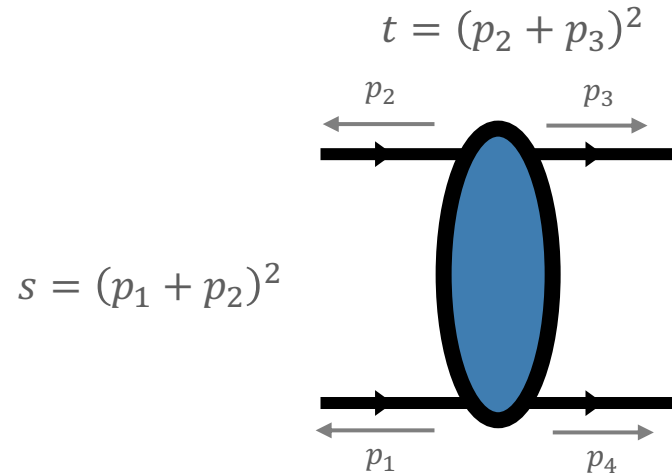
The background is a vibrant, abstract composition of various geometric shapes and colors. It includes a large light blue L-shaped figure in the top left, a yellow circle and a light blue ring with a white center in the top center, and a light green L-shaped figure in the top right. A horizontal light blue bar with a black border is positioned across the middle, containing the text. Below this bar, there are several other shapes: a purple triangle, a yellow triangle, and various black, orange, and light green lines and rectangles. The overall style is modern and graphic.

Part 1: QCD in the high-energy limit

HIGH-ENERGY LOGARITHMS

At each order in perturbative QCD, large logarithms arise when the centre of mass energy is much greater than the transverse momenta of the produced partons.

Consider the partonic cross section for inclusive dijet production:



$$L \equiv \log\left(\frac{s}{-t}\right) \gg 1$$

$$\alpha_s \ll 1$$

$$\alpha_s L \sim 1$$

$$\sigma^{(0)}/\sigma^{(0)} = 1$$

$$\sigma^{(1)}/\sigma^{(0)} = \alpha_s L c_0^{(1)} + \alpha_s c_1^{(1)}$$

$$\sigma^{(2)}/\sigma^{(0)} = \alpha_s^2 L^2 c_0^{(2)} + \alpha_s^2 L c_1^{(2)} + \alpha_s^2 c_2^{(2)}$$

$$\sigma^{(3)}/\sigma^{(0)} = \alpha_s^3 L^3 c_0^{(3)} + \alpha_s^3 L^2 c_1^{(3)} + \alpha_s^3 L c_2^{(3)} + \dots$$

$$\vdots$$

$$\vdots$$

$$\vdots$$

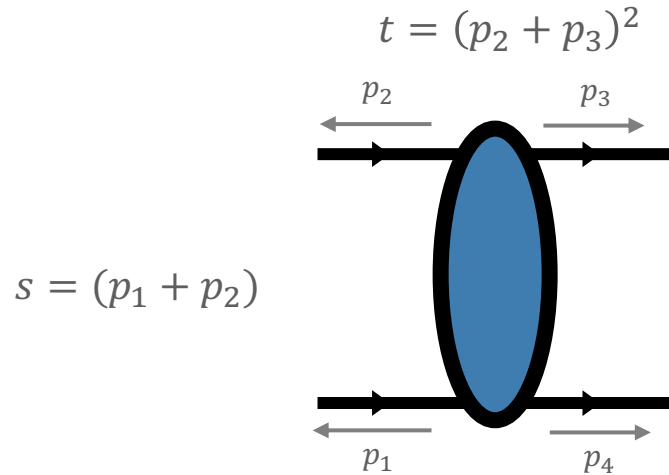
$$\vdots$$

We need to sum the whole tower of logarithms in order to restore stability to perturbative predictions.

HIGH-ENERGY LOGARITHMS

At each order in perturbative QCD, large logarithms arise when the centre of mass energy is much greater than the transverse momenta of the produced partons.

Consider the partonic cross section for inclusive dijet production:



$$L \equiv \log\left(\frac{s}{-t}\right) \gg 1$$

$$\alpha_s \ll 1$$

$$\alpha_s L \sim 1$$

$$\sigma^{(0)}/\sigma^{(0)} =$$

LL

1

$$\sigma^{(1)}/\sigma^{(0)} =$$

$$\alpha_s L c_0^{(1)}$$

+

$$\alpha_s c_1^{(1)}$$

$$\sigma^{(2)}/\sigma^{(0)} =$$

$$\alpha_s^2 L^2 c_0^{(2)}$$

+

$$\alpha_s^2 L c_1^{(2)}$$

+

$$\alpha_s^2 c_2^{(2)}$$

$$\sigma^{(3)}/\sigma^{(0)} =$$

$$\alpha_s^3 L^3 c_0^{(3)}$$

+

$$\alpha_s^3 L^2 c_1^{(3)}$$

+

$$\alpha_s^3 L c_2^{(3)}$$

+ ...

⋮

⋮

⋮

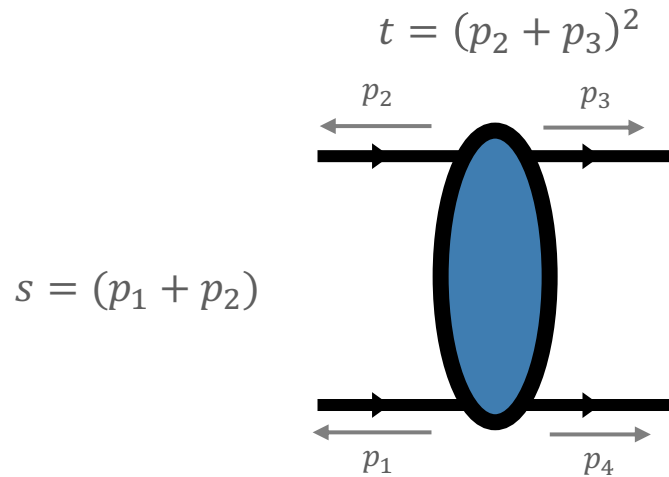
⋮

We need to sum the whole tower of logarithms in order to restore stability to perturbative predictions.

HIGH-ENERGY LOGARITHMS

At each order in perturbative QCD, large logarithms arise when the centre of mass energy is much greater than the transverse momenta of the produced partons.

Consider the partonic cross section for inclusive dijet production:



$$L \equiv \log\left(\frac{s}{-t}\right) \gg 1$$

$$\alpha_s \ll 1$$

$$\alpha_s L \sim 1$$

$$\sigma^{(0)}/\sigma^{(0)} =$$

LL

$$1$$

$$\sigma^{(1)}/\sigma^{(0)} =$$

$$\alpha_s L c_0^{(1)}$$

+

NLL

$$\alpha_s c_1^{(1)}$$

$$\sigma^{(2)}/\sigma^{(0)} =$$

$$\alpha_s^2 L^2 c_0^{(2)}$$

+

$$\alpha_s^2 L c_1^{(2)}$$

+

$$\alpha_s^2 c_2^{(2)}$$

$$\sigma^{(3)}/\sigma^{(0)} =$$

$$\alpha_s^3 L^3 c_0^{(3)}$$

+

$$\alpha_s^3 L^2 c_1^{(3)}$$

+

$$\alpha_s^3 L c_2^{(3)}$$

+ ...

⋮

⋮

⋮

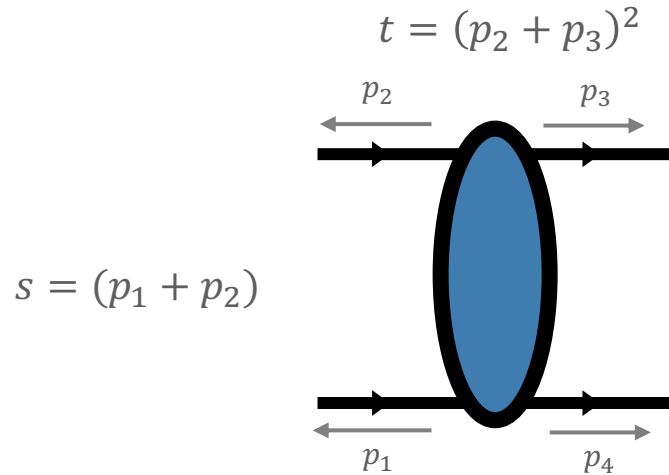
⋮

We need to sum the whole tower of logarithms in order to restore stability to perturbative predictions.

HIGH-ENERGY LOGARITHMS

At each order in perturbative QCD, large logarithms arise when the centre of mass energy is much greater than the transverse momenta of the produced partons.

Consider the partonic cross section for inclusive dijet production:



$$L \equiv \log\left(\frac{s}{-t}\right) \gg 1$$

$$\alpha_s \ll 1$$

$$\alpha_s L \sim 1$$

$$\sigma^{(0)}/\sigma^{(0)} =$$

LL

$$1$$

$$\sigma^{(1)}/\sigma^{(0)} =$$

$$\alpha_s L c_0^{(1)}$$

+

NLL

$$\alpha_s c_1^{(1)}$$

$$\sigma^{(2)}/\sigma^{(0)} =$$

$$\alpha_s^2 L^2 c_0^{(2)}$$

+

$$\alpha_s^2 L c_1^{(2)}$$

+

NNLL

$$\alpha_s^2 c_2^{(2)}$$

$$\sigma^{(3)}/\sigma^{(0)} =$$

$$\alpha_s^3 L^3 c_0^{(3)}$$

+

$$\alpha_s^3 L^2 c_1^{(3)}$$

+

$$\alpha_s^3 L c_2^{(3)}$$

+ ...

⋮

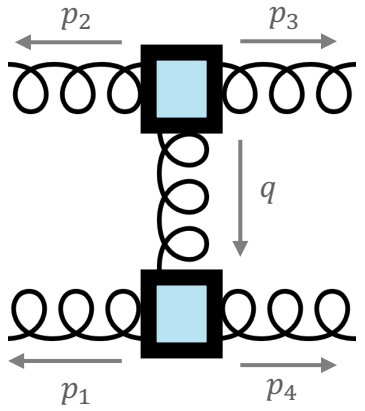
⋮

⋮

⋮

We need to sum the whole tower of logarithms in order to restore stability to perturbative predictions.

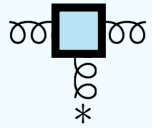
REGGE LIMIT OF 2→2 SCATTERING AT LO



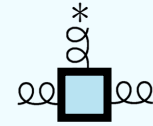
In the Regge limit the LO QCD amplitudes takes a simple factorised form:

$$\mathcal{M}_{gg \rightarrow gg}^{(0)} \xrightarrow{s \gg -t} 2s \mathcal{C}_{ggg^*}^{(0)}(p_2^{\lambda_2}, p_3^{\lambda_3}, q) \left(\frac{1}{|q_{\perp}|^2} \right) \mathcal{C}_{g^*gg}^{(0)}(-q, p_4^{\lambda_4}, p_1^{\lambda_1})$$

where the so-called impact factors are simple helicity conserving phases: [1]

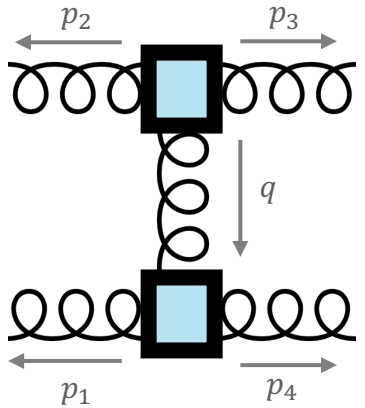


$$\mathcal{C}_{ggg^*}^{(0)}(p_2^{\oplus}, p_3^{\ominus}, q) = g_s f^{a_2 a_3 c} (1)$$



$$\mathcal{C}_{g^*gg}^{(0)}(-q, p_4^{\oplus}, p_1^{\ominus}) = g_s f^{a_4 a_1 c} \left(-\frac{p_{4\perp}^*}{p_{4\perp}} \right)$$

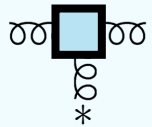
REGGE LIMIT OF 2→2 SCATTERING AT LO



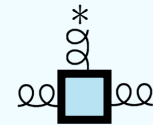
In the Regge limit the LO QCD amplitudes takes a simple factorised form:

$$\mathcal{M}_{gg \rightarrow gg}^{(0)} \xrightarrow{s \gg -t} 2s \mathcal{C}_{ggg^*}^{(0)}(p_2^{\lambda_2}, p_3^{\lambda_3}, q) \left(\frac{1}{|q_{\perp}|^2} \right) \mathcal{C}_{g^*gg}^{(0)}(-q, p_4^{\lambda_4}, p_1^{\lambda_1})$$

where the so-called impact factors are simple helicity conserving phases: [1]

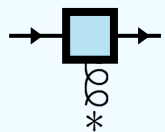


$$\mathcal{C}_{ggg^*}^{(0)}(p_2^{\oplus}, p_3^{\ominus}, q) = g_s f^{a_2 a_3 c} (1)$$

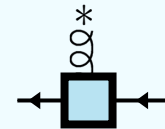


$$\mathcal{C}_{g^*gg}^{(0)}(-q, p_4^{\oplus}, p_1^{\ominus}) = g_s f^{a_4 a_1 c} \left(-\frac{p_{4\perp}^*}{p_{4\perp}} \right)$$

Quark scattering is similarly described, but with fundamental generators in place of the adjoint ones: [2]

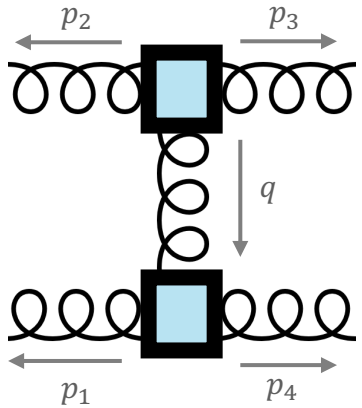


$$\mathcal{C}_{\bar{q}qg^*}^{(0)}(p_2^{\oplus}, p_3^{\ominus}, q) = g_s T_{i_3 i_2}^c (1)$$



$$\mathcal{C}_{g^*qg}^{(0)}(-q, p_4^{\oplus}, p_1^{\ominus}) = g_s T_{i_1 i_4}^c \left(\frac{p_{4\perp}^*}{p_{4\perp}} \right)^{\frac{1}{2}}$$

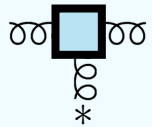
REGGE LIMIT OF 2→2 SCATTERING AT LO



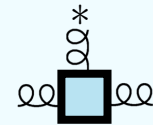
In the Regge limit the LO QCD amplitudes takes a simple factorised form:

$$\mathcal{M}_{gg \rightarrow gg}^{(0)} \xrightarrow{s \gg -t} 2s \mathcal{C}_{ggg^*}^{(0)}(p_2^{\lambda_2}, p_3^{\lambda_3}, q) \left(\frac{1}{|q_{\perp}|^2} \right) \mathcal{C}_{g^*gg}^{(0)}(-q, p_4^{\lambda_4}, p_1^{\lambda_1})$$

where the so-called impact factors are simple helicity conserving phases: [1]

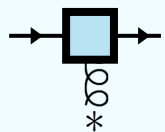


$$\mathcal{C}_{ggg^*}^{(0)}(p_2^{\oplus}, p_3^{\ominus}, q) = g_s f^{a_2 a_3 c} (1)$$

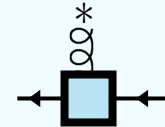


$$\mathcal{C}_{g^*gg}^{(0)}(-q, p_4^{\oplus}, p_1^{\ominus}) = g_s f^{a_4 a_1 c} \left(-\frac{p_{4\perp}^*}{p_{4\perp}} \right)$$

Quark scattering is similarly described, but with fundamental generators in place of the adjoint ones: [2]



$$\mathcal{C}_{\bar{q}qg^*}^{(0)}(p_2^{\oplus}, p_3^{\ominus}, q) = g_s T_{i_3 i_2}^c (1)$$



$$\mathcal{C}_{g^*\bar{q}q}^{(0)}(-q, p_4^{\oplus}, p_1^{\ominus}) = g_s T_{i_1 i_4}^c \left(\frac{p_{4\perp}^*}{p_{4\perp}} \right)^{\frac{1}{2}}$$

For all channels ($gg \rightarrow gg, qg \rightarrow qg, qQ \rightarrow qQ$ etc.), the leading-power amplitudes are described by antisymmetric octet exchange $\mathbf{8}_a$ in the t -channel, and have only a simple pole in $|q_{\perp}|^2$.

REGGE LIMIT OF 2→2 SCATTERING AT NLO

At loop level we might have expected other representations to be exchanged in the t -channel. For the example of $gg \rightarrow gg$ scattering, naively we might have expected any of the following representations,

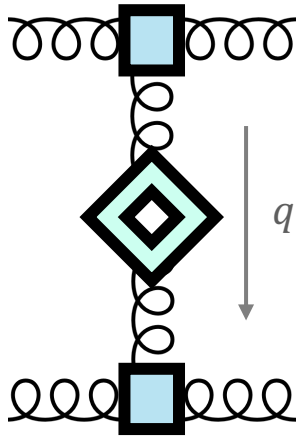
$$\mathbf{8}_a \otimes \mathbf{8}_a = \mathbf{1} \oplus \mathbf{8}_a \oplus \mathbf{8}_s \oplus \mathbf{10} \oplus \overline{\mathbf{10}} \oplus \mathbf{27}.$$

REGGE LIMIT OF 2→2 SCATTERING AT NLO

At loop level we might have expected other representations to be exchanged in the t -channel. For the example of $gg \rightarrow gg$ scattering, naively we might have expected any of the following representations,

$$\mathbf{8}_a \otimes \mathbf{8}_a = \mathbf{1} \oplus \mathbf{8}_a \oplus \mathbf{8}_s \oplus \mathbf{10} \oplus \overline{\mathbf{10}} \oplus \mathbf{27}.$$

However, in the Regge limit, the one-loop correction to the amplitude does not alter the colour structure:



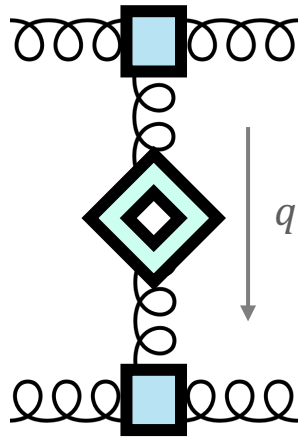
$$\begin{aligned} \mathcal{M}_{gg \rightarrow gg}^{(1)} \xrightarrow{s \gg -t} & 2s \mathcal{C}_{ggg^*}^{(0)}(p_2^{\lambda_2}, p_3^{\lambda_3}, q) \\ & \times \left(\frac{1}{|q_\perp|^2} \right) \alpha^{(1)}(q_\perp) \log \left(\frac{s}{|q_\perp|^2} \right) \\ & \times \mathcal{C}_{g^*gg}^{(0)}(-q, p_4^{\lambda_4}, p_1^{\lambda_1}) \end{aligned}$$

REGGE LIMIT OF 2→2 SCATTERING AT NLO

At loop level we might have expected other representations to be exchanged in the t -channel. For the example of $gg \rightarrow gg$ scattering, naively we might have expected any of the following representations,


$$\mathbf{8}_a \otimes \mathbf{8}_a = \mathbf{1} \oplus \mathbf{8}_a \oplus \mathbf{8}_s \oplus \mathbf{10} \oplus \overline{\mathbf{10}} \oplus \mathbf{27}.$$

However, in the Regge limit, the one-loop correction to the amplitude does not alter the colour structure:



$$\begin{aligned} \mathcal{M}_{gg \rightarrow gg}^{(1)} \xrightarrow{s \gg -t} & 2s \mathcal{C}_{ggg^*}^{(0)}(p_2^{\lambda_2}, p_3^{\lambda_3}, q) \\ & \times \left(\frac{1}{|q_\perp|^2} \right) \alpha^{(1)}(q_\perp) \log \left(\frac{s}{|q_\perp|^2} \right) \\ & \times \mathcal{C}_{g^*gg}^{(0)}(-q, p_4^{\lambda_4}, p_1^{\lambda_1}) \end{aligned}$$

The LL contribution from the loop integration appears with the transverse function known as the Regge trajectory [2]:

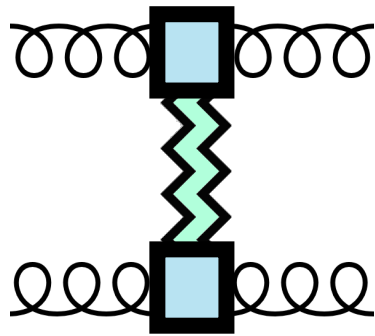


$$\alpha^{(1)}(q_\perp) \log \left(\frac{s}{|q_\perp|^2} \right), \quad \alpha^{(1)}(q_\perp) = g_s^2 \frac{\kappa_\Gamma}{4\pi} N_c \frac{2}{\epsilon} \left(\frac{\mu^2}{|q_\perp|^2} \right)^\epsilon$$

$$\kappa_\Gamma = (4\pi)^\epsilon \frac{\Gamma(1+\epsilon)\Gamma^2(1-\epsilon)}{\Gamma(1-2\epsilon)}$$

REGGE LIMIT OF 2→2 SCATTERING TO ALL ORDERS

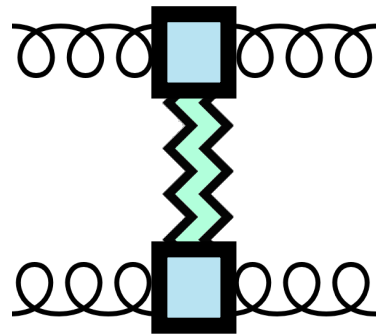
In the Regge limit, it is found that the virtual corrections simply exponentiate to all orders: [3]



$$\begin{aligned}
 \mathcal{M}_{f_1 f_2 \rightarrow f_3 f_4} \xrightarrow{s \gg -t} & 2s \mathcal{C}_{f_1 f_2 g^*}^{(0)}(p_2^{\lambda_2}, p_3^{\lambda_3}, q) \\
 & \times \left(\frac{1}{|q_\perp|^2} \right) e^{\alpha^{(1)}(q_\perp) \log\left(\frac{s}{|q_\perp|^2}\right)} \\
 & \times \mathcal{C}_{g^* f_4 f_1}^{(0)}(-q, p_4^{\lambda_4}, p_1^{\lambda_1})
 \end{aligned}$$

REGGE LIMIT OF 2→2 SCATTERING TO ALL ORDERS

In the Regge limit, it is found that the virtual corrections simply exponentiate to all orders: [3]



$$\mathcal{M}_{f_1 f_2 \rightarrow f_3 f_4} \xrightarrow{s \gg -t} 2s \mathcal{C}_{f_1 f_2 g^*}^{(0)}(p_2^{\lambda_2}, p_3^{\lambda_3}, q) \times \left(\frac{1}{|q_\perp|^2} \right) e^{\alpha^{(1)}(q_\perp) \log\left(\frac{s}{|q_\perp|^2}\right)} \times \mathcal{C}_{g^* f_4 f_1}^{(0)}(-q, p_4^{\lambda_4}, p_1^{\lambda_1})$$

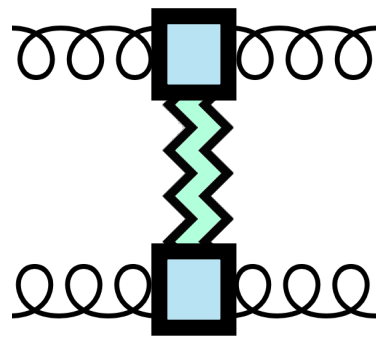
This exponential can be interpreted as a modification of the gluon propagator, known as gluon Reggeisation:

$$\left(\frac{1}{|q_\perp|^2} \right) \rightarrow \left(\frac{1}{|q_\perp|^2} \right) e^{\alpha^{(1)}(q_\perp)(y_3 - y_4)}$$

$$y_3 - y_4 = \frac{1}{2} \left(\log \left(\frac{p_3^+}{p_3^-} \right) - \log \left(\frac{p_4^+}{p_4^-} \right) \right) = \log \left(\frac{p_3^+ p_4^-}{|q_\perp|^2} \right) \xrightarrow{s \gg -t} \log \left(\frac{s_{34}}{|q_\perp|^2} \right)$$

REGGE LIMIT OF 2→2 SCATTERING TO ALL ORDERS

In the Regge limit, it is found that the virtual corrections simply exponentiate to all orders: [3]



$$\mathcal{M}_{f_1 f_2 \rightarrow f_3 f_4} \xrightarrow{s \gg -t} 2s \mathcal{C}_{f_1 f_2 g^*}^{(0)}(p_2^{\lambda_2}, p_3^{\lambda_3}, q) \times \left(\frac{1}{|q_\perp|^2} \right) e^{\alpha^{(1)}(q_\perp) \log\left(\frac{s}{|q_\perp|^2}\right)} \times \mathcal{C}_{g^* f_4 f_1}^{(0)}(-q, p_4^{\lambda_4}, p_1^{\lambda_1})$$

This exponential can be interpreted as a modification of the gluon propagator, known as gluon Reggeisation:

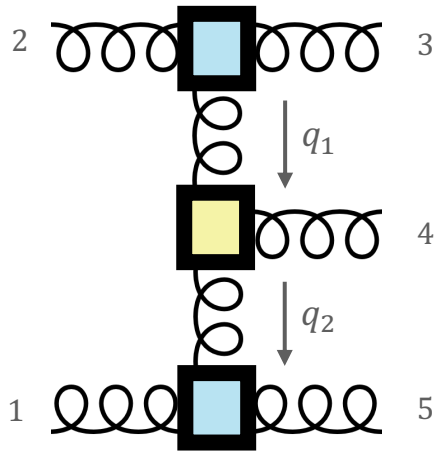
$$\begin{aligned} \begin{array}{c} * \\ \text{Zigzag} \\ * \end{array} \left(\frac{1}{|q_\perp|^2} \right) &\rightarrow \left(\frac{1}{|q_\perp|^2} \right) e^{\alpha^{(1)}(q_\perp)(y_3 - y_4)} & y_3 - y_4 &= \frac{1}{2} \left(\log\left(\frac{p_3^+}{p_3^-}\right) - \log\left(\frac{p_4^+}{p_4^-}\right) \right) \\ & & &= \log\left(\frac{p_3^+ p_4^-}{|q_\perp|^2}\right) \xrightarrow{s \gg -t} \log\left(\frac{s_{34}}{|q_\perp|^2}\right) \end{aligned}$$

In order to find the LL behaviour of the cross section we must also study real emissions.

REGGE LIMIT OF 2→3 SCATTERING AT LO

The LL contribution from the phase-space integration of an additional real emission comes from the Multi-Regge Kinematic (MRK) region:

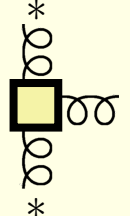
$$y_3 \gg y_4 \gg y_5, \quad |p_{3\perp}| \approx |p_{4\perp}| \approx |p_{5\perp}|$$



At LO the amplitude again has a simple factorised form:

$$\begin{aligned} \mathcal{M}_{gg \rightarrow ggg}^{(0)} \xrightarrow{\text{MRK}} & 2s \mathcal{C}_{ggg^*}^{(0)}(p_2^{\lambda_2}, p_3^{\lambda_3}, q_1) \\ & \times \left(\frac{1}{|q_{1\perp}|^2} \right) \times \mathcal{V}_{g^*gg^*}^{(0)}(-q_1, p_4, q_2) \times \left(\frac{1}{|q_{2\perp}|^2} \right) \\ & \times \mathcal{C}_{g^*gg}^{(0)}(-q_2, p_5^{\lambda_5}, p_1^{\lambda_1}) \end{aligned}$$

where the contribution of all gluon emissions is given by the effective Lipatov vertex [2]:

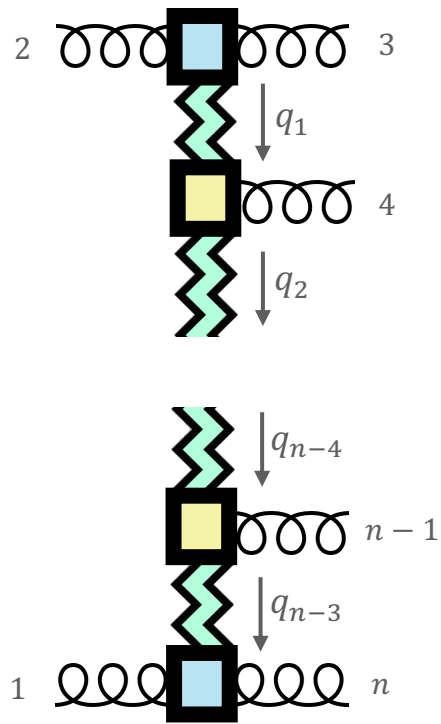


$$\mathcal{V}_{g^*gg^*}^{(0)}(-q_1, p_4^\oplus, q_2) = g_s f^{c_1 a_4 c_2} \frac{q_{1\perp}^* q_{2\perp}}{p_{4\perp}}$$

Again, we see that the amplitude is governed by the exchange of gluon quantum numbers in the t_1 and t_2 channels.

THE REGGE LIMIT OF QCD TO LL

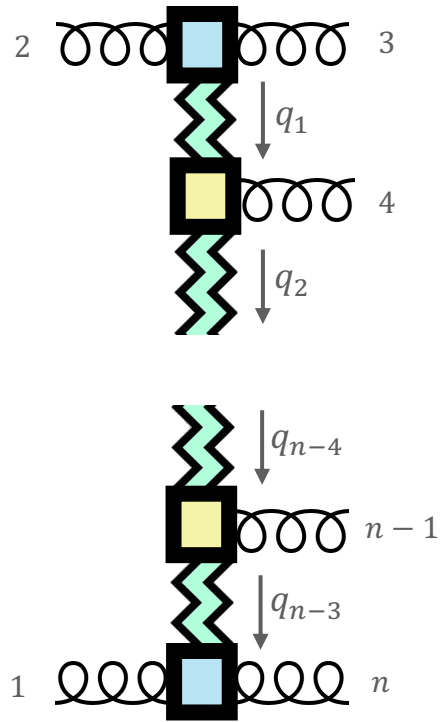
The $2 \rightarrow n$ amplitude in QCD is described to all orders by: [3]



$$\begin{aligned}
 \mathcal{M}_{f_1 f_2 \rightarrow f_3 f_n + (n-2)g} \Big|_{\text{LL}} &= 2s_{12} \mathcal{C}_{f_1 f_2 g^*}^{(0)}(p_2^{\nu_2}, p_3^{-\nu_2}, q_1) \\
 &\times \prod_{i=4}^{n-1} \mathcal{V}_{g^* g g^*}^{(0)}(q_{i-3}, p_i^{\nu_i}, q_{i-2}) \\
 &\times \prod_{i=1}^{n-3} \frac{1}{|q_{i\perp}|^2} e^{\alpha^{(1)}(q_{i\perp})(y_{i+2} - y_{i+3})} \\
 &\times \mathcal{C}_{g^* f_n f_1}^{(0)}(q_{n-3}, p_n^{-\nu_1}, p_1^{\nu_1},)
 \end{aligned}$$

THE REGGE LIMIT OF QCD TO LL

The $2 \rightarrow n$ amplitude in QCD is described to all orders by: [3]



$$\begin{aligned}
 \mathcal{M}_{f_1 f_2 \rightarrow f_3 f_n + (n-2)g} \Big|_{\text{LL}} &= 2s_{12} \mathcal{C}_{f_1 f_2 g^*}^{(0)}(p_2^{\nu_2}, p_3^{-\nu_2}, q_1) \\
 &\times \prod_{i=4}^{n-1} \mathcal{V}_{g^* g g^*}^{(0)}(q_{i-3}, p_i^{\nu_i}, q_{i-2}) \\
 &\times \prod_{i=1}^{n-3} \frac{1}{|q_{i\perp}|^2} e^{\alpha^{(1)}(q_{i\perp})(y_{i+2} - y_{i+3})} \\
 &\times \mathcal{C}_{g^* f_n f_1}^{(0)}(q_{n-3}, p_n^{-\nu_1}, p_1^{\nu_1},)
 \end{aligned}$$

This was the form from which the BFKL equation was first derived [4].

This observation is also the starting point of HEJ, although from this point the two approaches diverge.

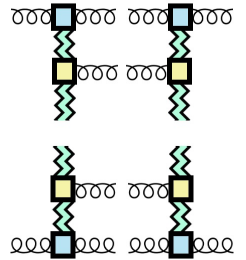
We would like to clarify how these approaches differ in the treatment of logarithmic corrections to the cross section within collinear factorisation.

$$\sigma_{AB \rightarrow X} = \sum_{f_1, f_2} \int_0^1 dx_1 dx_2 f_{f_1/A}(x_1) f_{f_2/B}(x_2) \hat{\sigma}_{f_1 f_2}$$

COMPARISON OF BFKL AND HEJ

One way to derive the BFKL equation is to combine the Regge-factorised amplitudes with *s-channel unitarity* [5]

$$\text{Disc}_s [\overline{\mathcal{M}}_{f_1 f_2 \rightarrow f'_1 f'_2}(s, t = 0)] = \frac{1}{2} \sum_{n=4}^{\infty} \sum_{f_i, a_i, \lambda_i} \int d\Phi_{n-2} \mathcal{M}_{f_1 f_2 \rightarrow f_3 \dots f_n} (\mathcal{M}_{f'_1 f'_2 \rightarrow f_3 \dots f_n})^*$$



COMPARISON OF BFKL AND HEJ

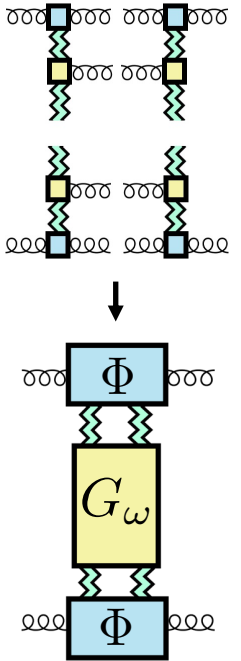
One way to derive the BFKL equation is to combine the Regge-factorised amplitudes with *s-channel unitarity* [5]

$$\text{Disc}_s [\overline{\mathcal{M}}_{f_1 f_2 \rightarrow f'_1 f'_2}(s, t = 0)] = \frac{1}{2} \sum_{n=4}^{\infty} \sum_{f_i, a_i, \lambda_i} \int d\Phi_{n-2} \mathcal{M}_{f_1 f_2 \rightarrow f_3 \dots f_n} (\mathcal{M}_{f'_1 f'_2 \rightarrow f_3 \dots f_n})^*$$

A Mellin transform allows the longitudinal integrals to be performed analytically over MRK phase space.

The central physics is captured by the gluon Green's function, G_ω , which obeys a recursive integral equation. For the case of forward scattering and vacuum quantum numbers, this is the BFKL equation [4], which can be solved analytically. The partonic cross section can be written

$$\hat{\sigma}_{f_1 f_2}(s) = \int_{\delta-i\infty}^{\delta+i\infty} \frac{d\omega}{2\pi i} \int d^{D-2} q_{1\perp} d^{D-2} q_{(n-3)\perp} \left(\frac{s}{s_0}\right)^\omega \times \frac{\Phi_{f_2}(\vec{q}_1)}{\vec{q}_1^2} \times G_\omega(\vec{q}_1, \vec{q}_{(n-3)}) \times \frac{\Phi_{f_1}(-\vec{q}_{(n-3)})}{\vec{q}_{(n-3)}^2}$$



COMPARISON OF BFKL AND HEJ

One way to derive the BFKL equation is to combine the Regge-factorised amplitudes with *s-channel unitarity* [5]

$$\text{Disc}_s [\overline{\mathcal{M}}_{f_1 f_2 \rightarrow f'_1 f'_2}(s, t=0)] = \frac{1}{2} \sum_{n=4}^{\infty} \sum_{f_i, a_i, \lambda_i} \int d\Phi_{n-2} \mathcal{M}_{f_1 f_2 \rightarrow f_3 \dots f_n} (\mathcal{M}_{f'_1 f'_2 \rightarrow f_3 \dots f_n})^*$$

A Mellin transform allows the longitudinal integrals to be performed analytically over MRK phase space.

The central physics is captured by the gluon Green's function, G_ω , which obeys a recursive integral equation. For the case of forward scattering and vacuum quantum numbers, this is the BFKL equation [4], which can be solved analytically. The partonic cross section can be written

$$\hat{\sigma}_{f_1 f_2}(s) = \int_{\delta-i\infty}^{\delta+i\infty} \frac{d\omega}{2\pi i} \int d^{D-2} q_{1\perp} d^{D-2} q_{(n-3)\perp} \left(\frac{s}{s_0}\right)^\omega \times \frac{\Phi_{f_2}(\vec{q}_1)}{\vec{q}_1^2} \times G_\omega(\vec{q}_1, \vec{q}_{(n-3)}) \times \frac{\Phi_{f_1}(-\vec{q}_{(n-3)})}{\vec{q}_{(n-3)}^2}$$

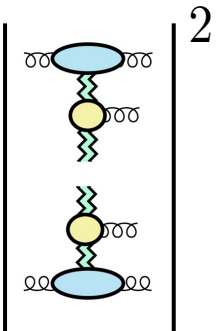
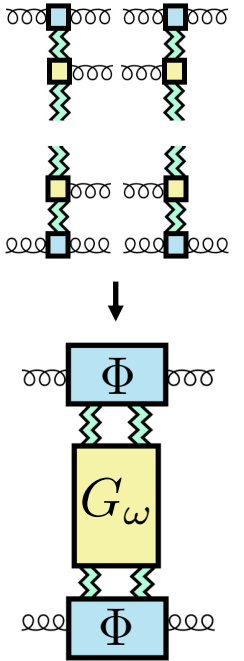
On the other hand, the starting point of HEJ [6] is to only use a Regge-factorised approximation to amplitudes to compute the partonic cross section *directly*:

$$\hat{\sigma}_{f_1 f_2} = \int d\Phi_X \frac{|\mathcal{M}_{f_1 f_2 \rightarrow X}|^2}{2\hat{s}}$$

There are many benefits to performing the phase space numerically, not least the fact that the momentum fractions can be reconstructed exactly.

$$x_{f_1} = \frac{1}{\sqrt{s_{\text{had}}}} \left(\sum_{i=3}^n |p_{i\perp}| e^{y_i} \right) \xrightarrow{\text{LL}} \frac{|p_{3\perp}|}{\sqrt{s_{\text{had}}}} e^{y_3}$$

Other benefits: LO matching, exclusive observables, cuts, interfacing with standard HE tools such as Rivet.



The background is a vibrant, abstract composition of various geometric shapes and colors. It includes a large light blue L-shaped figure in the top left, a large light blue circle with a smaller white circle inside in the top center, a light green L-shaped figure in the top right, a purple triangle in the middle, and several other shapes in shades of blue, green, yellow, and orange. The shapes are scattered across the white background, creating a dynamic and colorful pattern.

Part 2: Amplitudes in HEJ

2→2 AT LO REVISITED: QUARK SCATTERING

Consider the Feynman diagrams for the scattering of $qQ \rightarrow qQ$. Only a single diagram contributes:

$$\mathcal{M}_{qQ \rightarrow qQ} = [ig_s T_{i_3 \bar{i}_2}^{a_A} \bar{u}(p_3) \gamma^{\mu_A} u(-p_2)] \times \left[\frac{-ig_{\mu_A \mu_B} \delta^{a_A a_B}}{t} \right] \times [ig_s T_{i_4 \bar{i}_1}^{a_B} \bar{u}(p_4) \gamma^{\mu_B} u(-p_1)]$$

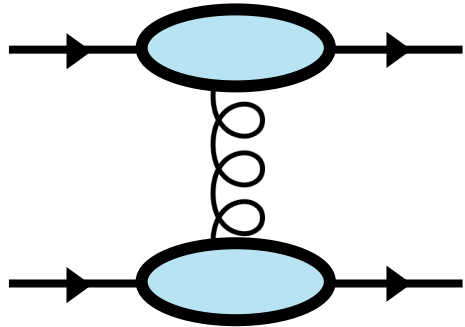
We see that the amplitude already has the high-energy factorised form, *without any kinematic approximations*.

2→2 AT LO REVISITED: QUARK SCATTERING

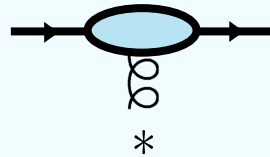
Consider the Feynman diagrams for the scattering of $qQ \rightarrow qQ$. Only a single diagram contributes:

$$\mathcal{M}_{qQ \rightarrow qQ} = [ig_s T_{i_3 \bar{i}_2}^{a_A} \bar{u}(p_3) \gamma^{\mu_A} u(-p_2)] \times \left[\frac{-ig_{\mu_A \mu_B} \delta^{a_A a_B}}{t} \right] \times [ig_s T_{i_4 \bar{i}_1}^{a_B} \bar{u}(p_4) \gamma^{\mu_B} u(-p_1)]$$

We see that the amplitude already has the high-energy factorised form, *without any kinematic approximations*.



This motivates us to take the impact factors to be the full quark currents: [7,8]



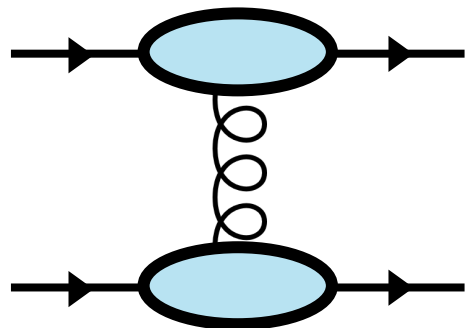
$$C_{\bar{q}qg^*}^{\mu(0)}(p_2^\oplus, p_3^\ominus, q) = g_s T_{i_3 i_2}^c \langle 3 | \sigma^\mu | 2 \rangle$$

2→2 AT LO REVISITED: QUARK SCATTERING

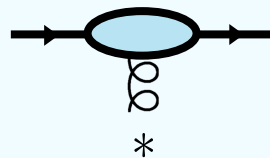
Consider the Feynman diagrams for the scattering of $qQ \rightarrow qQ$. Only a single diagram contributes:

$$\mathcal{M}_{qQ \rightarrow qQ} = [ig_s T_{i_3 i_2}^{a_A} \bar{u}(p_3) \gamma^{\mu_A} u(-p_2)] \times \left[\frac{-ig_{\mu_A \mu_B} \delta^{a_A a_B}}{t} \right] \times [ig_s T_{i_4 i_1}^{a_B} \bar{u}(p_4) \gamma^{\mu_B} u(-p_1)]$$

We see that the amplitude already has the high-energy factorised form, *without any kinematic approximations*.



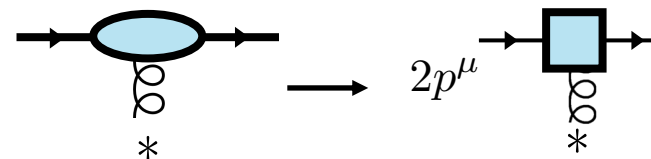
This motivates us to take the impact factors to be the full quark currents: [7,8]



$$C_{\bar{q}qg^*}^{\mu(0)}(p_2^{\oplus}, p_3^{\ominus}, q) = g_s T_{i_3 i_2}^c \langle 3 | \sigma^\mu | 2 \rangle$$

Note that the two forms of the impact factor agree in the strict high-energy limit:

$$g_s T_{i_3 i_2}^c \langle 3 | \sigma^\mu | 2 \rangle \xrightarrow{p_2^+ \sim p_3^+ \gg p_3^-} 2p_2^\mu g_s T_{i_3 i_2}^c e^{i\phi}$$

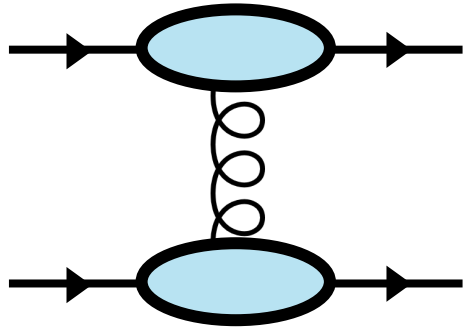


2→2 AT LO REVISITED: QUARK SCATTERING

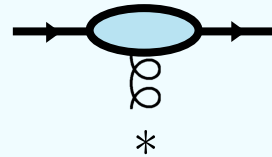
Consider the Feynman diagrams for the scattering of $qQ \rightarrow qQ$. Only a single diagram contributes:

$$\mathcal{M}_{qQ \rightarrow qQ} = [ig_s T_{i_3 \bar{i}_2}^{a_A} \bar{u}(p_3) \gamma^{\mu_A} u(-p_2)] \times \left[\frac{-ig_{\mu_A \mu_B} \delta^{a_A a_B}}{t} \right] \times [ig_s T_{i_4 \bar{i}_1}^{a_B} \bar{u}(p_4) \gamma^{\mu_B} u(-p_1)]$$

We see that the amplitude already has the high-energy factorised form, *without any kinematic approximations*.



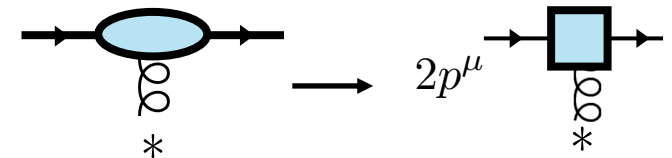
This motivates us to take the impact factors to be the full quark currents: [7,8]



$$C_{\bar{q}qg^*}^{\mu(0)}(p_2^{\oplus}, p_3^{\ominus}, q) = g_s T_{i_3 i_2}^c \langle 3 | \sigma^\mu | 2 \rangle$$

Note that the two forms of the impact factor agree in the strict high-energy limit:

$$g_s T_{i_3 i_2}^c \langle 3 | \sigma^\mu | 2 \rangle \xrightarrow{p_2^+ \sim p_3^+ \gg p_3^-} 2p_2^\mu g_s T_{i_3 i_2}^c e^{i\phi}$$



Note also that the full 4-dimensional pole in t can be retained. We do not have to approximate $\frac{1}{t} \rightarrow \frac{1}{|q_\perp|^2}$.

LO 2→2 REVISITED: GLUON SCATTERING

Consider the *colour-ordered* amplitudes for $qg \rightarrow qg$. These are related to the $qQ \rightarrow qQ$ amplitude by a supersymmetric Ward identity:

$$M_{gg\bar{q}q}^{(0)}(p_2^\oplus, p_3^\ominus, p_4^\oplus, p_1^\ominus) = \frac{\langle 13 \rangle}{\langle 12 \rangle} M_{\bar{Q}Q\bar{q}q}^{(0)}(p_2^\oplus, p_3^\ominus, p_4^\oplus, p_1^\ominus)$$

LO 2→2 REVISITED: GLUON SCATTERING

Consider the *colour-ordered* amplitudes for $qg \rightarrow qg$. These are related to the $qQ \rightarrow qQ$ amplitude by a supersymmetric Ward identity:

$$M_{gg\bar{q}q}^{(0)}(p_2^\oplus, p_3^\ominus, p_4^\oplus, p_1^\ominus) = \frac{\langle 13 \rangle}{\langle 12 \rangle} M_{\bar{Q}Q\bar{q}q}^{(0)}(p_2^\oplus, p_3^\ominus, p_4^\oplus, p_1^\ominus)$$

It follows that each colour-ordered amplitude can be written in the Regge-factorised form, *without any kinematic approximations*. We can therefore define the following *colour-ordered impact factors*:

$$C_{ggg^*}^{\mu(0)}(p_2^\oplus, p_3^\ominus, q) = \left(-\sqrt{\frac{p_3^+}{p_2^+}} \frac{p_{3\perp}^*}{p_{3\perp}} \right) \langle 3|\sigma^\mu|2] \quad C_{ggg^*}^{\mu(0)}(p_3^\ominus, p_2^\oplus, q) = \left(\sqrt{\frac{p_2^+}{p_3^+}} \frac{p_{3\perp}^*}{p_{3\perp}} \right) \langle 3|\sigma^\mu|2]$$

LO 2→2 REVISITED: GLUON SCATTERING

Consider the *colour-ordered* amplitudes for $qg \rightarrow qg$. These are related to the $qQ \rightarrow qQ$ amplitude by a supersymmetric Ward identity:

$$M_{gg\bar{q}q}^{(0)}(p_2^\oplus, p_3^\ominus, p_4^\oplus, p_1^\ominus) = \frac{\langle 13 \rangle}{\langle 12 \rangle} M_{\bar{Q}Q\bar{q}q}^{(0)}(p_2^\oplus, p_3^\ominus, p_4^\oplus, p_1^\ominus)$$

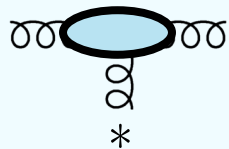
It follows that each colour-ordered amplitude can be written in the Regge-factorised form, *without any kinematic approximations*. We can therefore define the following *colour-ordered impact factors*:

$$C_{ggg^*}^{\mu(0)}(p_2^\oplus, p_3^\ominus, q) = \left(-\sqrt{\frac{p_3^+ p_{3\perp}^*}{p_2^+ p_{3\perp}}} \right) \langle 3|\sigma^\mu|2 \rangle \quad C_{ggg^*}^{\mu(0)}(p_2^\oplus, p_3^\ominus, q) = \left(-\sqrt{\frac{p_2^+ p_{3\perp}^*}{p_3^+ p_{3\perp}}} \right) \langle 3|\sigma^\mu|2 \rangle$$

Now considering the colour-dressed amplitude,

$$\mathcal{M}_{gg\bar{q}q}^{(0)}(p_2^\oplus, p_3^\ominus, p_4^\oplus, p_1^\ominus) = g_s^2 (T^{a_2} T^{a_3})_{i_1 i_4} M_{gg\bar{q}q}^{(0)}(p_2^\oplus, p_3^\ominus, p_4^\oplus, p_1^\ominus) + g_s^2 (T^{a_3} T^{a_2})_{i_1 i_4} M_{gg\bar{q}q}^{(0)}(p_3^\ominus, p_2^\oplus, p_4^\oplus, p_1^\ominus)$$

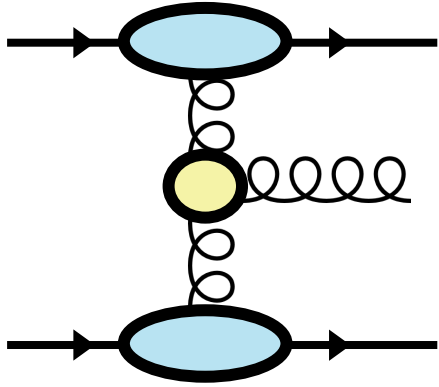
we see that only the antisymmetric combination of the colour factors is leading in the Regge limit. This defines the HEJ gluon current:



$$C_{ggg^*}^{\mu(0)}(p_2^\oplus, p_3^\ominus, q) = g_s f^{a_2 a_3 c} \frac{1}{2} \left(C_{ggg^*}^{\mu(0)}(p_2^\oplus, p_3^\ominus, q) + C_{ggg^*}^{\mu(0)}(p_3^\ominus, p_2^\oplus, q) \right)$$

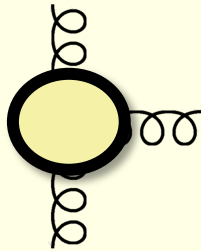
For $qg \rightarrow qg$, the colour-octet component of the LO amplitude is described exactly.

LO 2→3 REVISITED



By making minimal approximations to the amplitude for $q\bar{q} \rightarrow qg\bar{q}$, it is possible to derive a form of the Lipatov vertex which retains much of the information about the LO amplitude: [8]

$$\mathcal{M}_{q_1 q_2 \rightarrow q_1 q_2} = C_{\bar{q}qg^*}^{\mu_1(0)}(p_2^{\lambda_2}, p_3^{-\lambda_2}, q_1) \times \left(\frac{i}{t_1}\right) \times \mathcal{V}_{g^*gg^*}^{(0)\mu_1\mu_2}(p_4^{\lambda_4}) \times \left(\frac{i}{t_2}\right) \times C_{g^*q\bar{q}}^{\mu_2(0)}(-q_2, p_5^{-\lambda_1}, p_1^{\lambda_1})$$

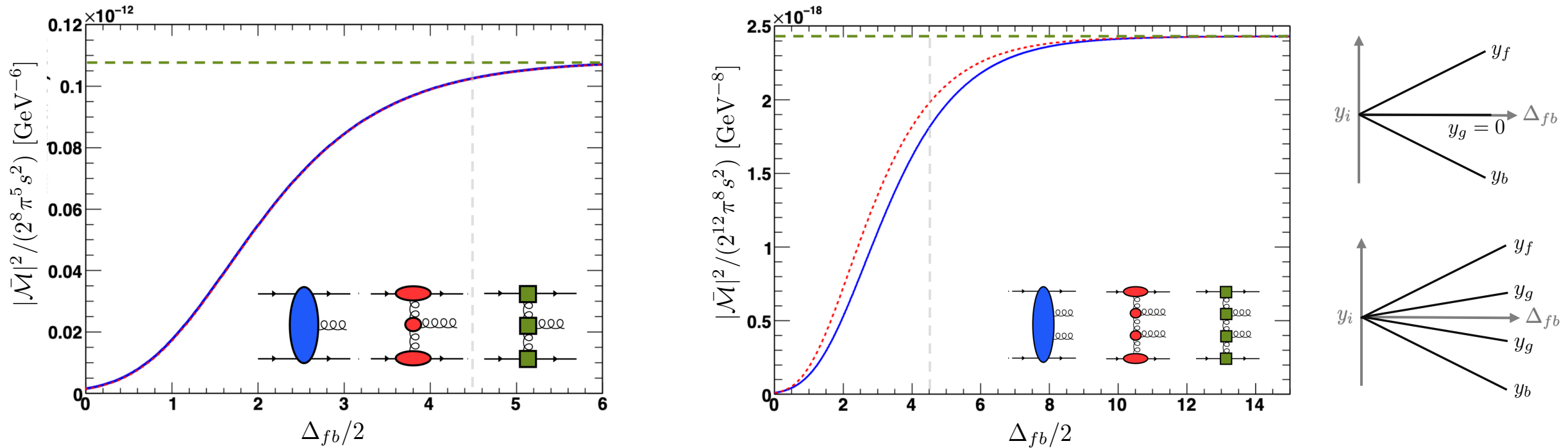


$$\begin{aligned} \mathcal{V}_{g^*gg^*}^{\mu_1\mu_2(0)}(-p_{t_1}, p_g^{\lambda_g}, p_{t_2}) &= \eta^{\mu_1\mu_2} \frac{ig_s}{2T_F} f^{a_{t_1} a_{t_2} a_g} \epsilon_{\mu_g} (p_g^{\lambda_g}, p_r) \\ &\times \left[(p_{t_1} + p_{t_2})^{\mu_g} - \frac{t_1}{2} \left(\frac{2p_{\bar{q}_1}^{\mu_g}}{s_{\bar{q}_1 g}} + \frac{2p_{q_1}^{\mu_g}}{s_{q_1 g}} \right) + \frac{t_2}{2} \left(\frac{2p_{\bar{q}_2}^{\mu_g}}{s_{\bar{q}_2 g}} + \frac{2p_{q_2}^{\mu_g}}{s_{q_2 g}} \right) + \right. \\ &\left. + \frac{1}{2} \left\{ \frac{s_{q_1 g} p_{q_2}^{\mu_g} - s_{q_2 g} p_{q_1}^{\mu_g}}{s_{q_1 q_2}} + \frac{s_{\bar{q}_1 g} p_{q_2}^{\mu_g} - s_{q_2 g} p_{\bar{q}_1}^{\mu_g}}{s_{\bar{q}_1 q_2}} + \frac{s_{q_1 g} p_{\bar{q}_2}^{\mu_g} - s_{\bar{q}_2 g} p_{q_1}^{\mu_g}}{s_{q_1 \bar{q}_2}} + \frac{s_{\bar{q}_1 g} p_{\bar{q}_2}^{\mu_g} - s_{\bar{q}_2 g} p_{\bar{q}_1}^{\mu_g}}{s_{\bar{q}_1 \bar{q}_2}} \right\} \right] \end{aligned}$$

This vertex is gauge invariant in all of phase space, not just the MKR limit. It conserves 4-momentum, not just transverse momentum. The vertex is symmetric with respect to $-p_2 \leftrightarrow p_3$ and $-p_1 \leftrightarrow p_4$ which better approximates the pole structure of the LO amplitude.

LO NUMERICAL COMPARISON

Comparing the two factorised approximations to amplitudes, we see the HEJ amplitudes capture much of the LO physics:

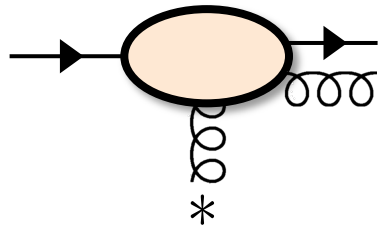


We see that the HEJ approximation to the LO matrix element is reasonable, even within LHC phase space. Integrating the strict approximation would lead to a massive overestimate of the cross section.

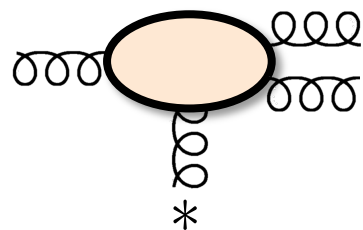
Of course, HEJ matrix elements are matched point-by-point to LO matrix elements where they are available.

REAL NLL CORRECTIONS IN HEJ

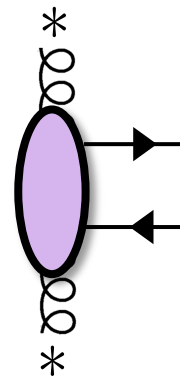
In order to move to NLL accuracy, we need both real and virtual corrections to the building blocks. We have recently completed the calculation of the real corrections with the minimal-approximation approach of HEJ:



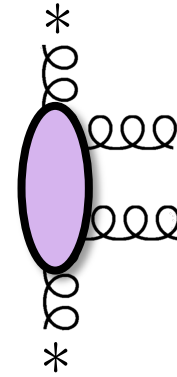
[9] 1706.01002



[via sWard]



[10] 2012.10310



[In preparation]

Regulating the IR divergences of these improved vertices requires almost all of the machinery of a NLO calculation. We are using a minimally modified FKS subtraction to perform this regularisation.

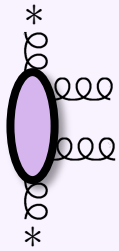
In the meantime, we can use these factorised expressions to improve the accuracy of HEJ by imposing jet clustering requirements to regulate IR divergences.

CENTRAL $g^* g g g^*$ VERTEX

The final ingredient we need is a central gg vertex. After minimal gauge invariant approximations, we find

$$\mathcal{M}(\bar{q}_1, q_1, g_1, g_2, \bar{q}_2, q_2) \xrightarrow{\text{NMRK}} \mathcal{C}_{\bar{q}qg^*\mu_{t_1}}^{a_{t_1}}(p_{\bar{q}_1}, p_{q_1}, p_{t_1}) \left(\frac{-i}{t_1}\right) \times \mathcal{V}_{g^*g g g^*}^{\mu_{t_1}\mu_{t_3} a_{t_1} a_{t_3}}(-p_{t_1}, p_{g_1}, p_{g_2}, p_{t_3}) \times \left(\frac{-i}{t_3}\right) \mathcal{C}_{\bar{q}qg^*\mu_{t_3}}(p_{\bar{q}_2}, p_{q_2}, -p_{t_3})$$

with vertex:



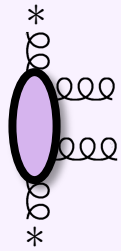
$$\begin{aligned} \mathcal{V}_{g^*g g g^*}^{\mu_{t_1}\mu_{t_3} a_{t_1} a_{t_3}}(-p_{t_1}, p_{g_1}, p_{g_2}, p_{t_3}) = & \sum_{\sigma \in S_2} \text{tr}(T^{a_{t_1}} T^{a_{t_3}} T^{a_{\sigma_1}} T^{a_{\sigma_2}}) V_{g^*g^*g g}^{\mu_{t_1}\mu_{t_3}}(-p_{t_1}, p_{t_3}, p_{g_{\sigma_1}}, p_{g_{\sigma_2}}) \\ & + \text{tr}(T^{a_{t_1}} T^{a_{\sigma_1}} T^{a_{\sigma_2}} T^{a_{t_3}}) V_{g^*g g g^*}^{\mu_{t_1}\mu_{t_3}}(-p_{t_1}, p_{g_{\sigma_1}}, p_{g_{\sigma_2}}, p_{t_3}) \\ & + \text{tr}(T^{a_{t_1}} T^{a_{\sigma_2}} T^{a_{t_3}} T^{a_{\sigma_1}}) V_{g^*g g^*g}^{\mu_{t_1}\mu_{t_3}}(-p_{t_1}, p_{g_{\sigma_2}}, p_{t_3}, p_{g_{\sigma_2}}). \end{aligned}$$

CENTRAL $g^* g g g^*$ VERTEX

The final ingredient we need is a central $g g$ vertex. After minimal gauge invariant approximations, we find

$$\mathcal{M}(\bar{q}_1, q_1, g_1, g_2, \bar{q}_2, q_2) \xrightarrow{\text{NMRK}} \mathcal{C}_{\bar{q} q g^* \mu_{t_1}}^{a_{t_1}}(p_{\bar{q}_1}, p_{q_1}, p_{t_1}) \left(\frac{-i}{t_1} \right) \times \mathcal{V}_{g^* g g g^*}^{\mu_{t_1} \mu_{t_3} a_{t_1} a_{t_3}}(-p_{t_1}, p_{g_1}, p_{g_2}, p_{t_3}) \times \left(\frac{-i}{t_3} \right) \mathcal{C}_{\bar{q} q g^* \mu_{t_3}}(p_{\bar{q}_2}, p_{q_2}, -p_{t_3})$$

with vertex:



$$\begin{aligned} \mathcal{V}_{g^* g g g^*}^{\mu_{t_1} \mu_{t_3} a_{t_1} a_{t_3}}(-p_{t_1}, p_{g_1}, p_{g_2}, p_{t_3}) &= \sum_{\sigma \in S_2} \text{tr}(T^{a_{t_1}} T^{a_{t_3}} T^{a_{\sigma_1}} T^{a_{\sigma_2}}) V_{g^* g^* g g}^{\mu_{t_1} \mu_{t_3}}(-p_{t_1}, p_{t_3}, p_{g_{\sigma_1}}, p_{g_{\sigma_2}}) \\ &+ \text{tr}(T^{a_{t_1}} T^{a_{\sigma_1}} T^{a_{\sigma_2}} T^{a_{t_3}}) V_{g^* g g g^*}^{\mu_{t_1} \mu_{t_3}}(-p_{t_1}, p_{g_{\sigma_1}}, p_{g_{\sigma_2}}, p_{t_3}) \\ &+ \text{tr}(T^{a_{t_1}} T^{a_{\sigma_2}} T^{a_{t_3}} T^{a_{\sigma_1}}) V_{g^* g g^* g}^{\mu_{t_1} \mu_{t_3}}(-p_{t_1}, p_{g_{\sigma_2}}, p_{t_3}, p_{g_{\sigma_1}}). \end{aligned}$$

which is written in terms of the colour-ordered vertices:

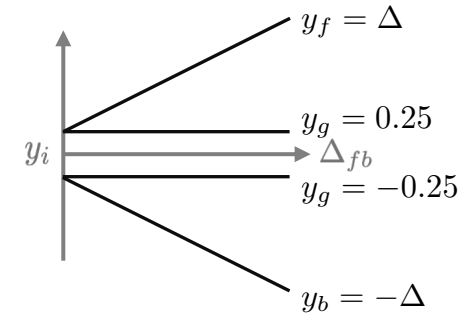
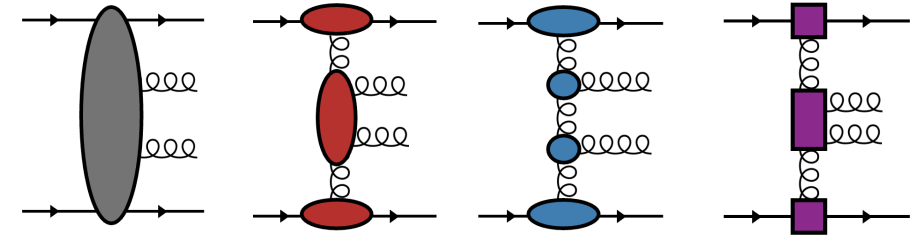
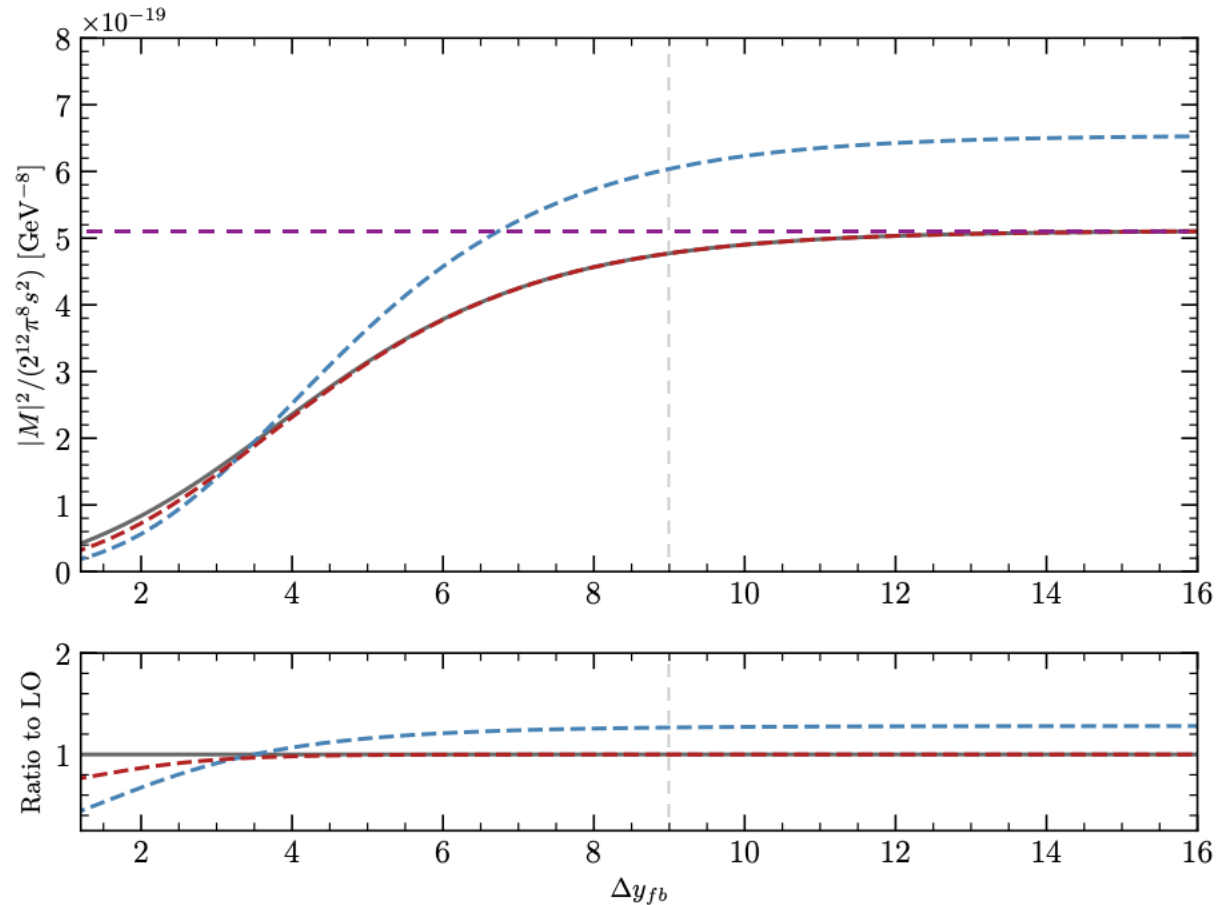
$$\begin{aligned} V_{g^* g g g^*}^{\mu_{t_1} \mu_{t_3}}(-p_{t_1}, p_{g_1}, p_{g_2}, p_{t_2}) &= i g_s \epsilon_{\mu_{g_1}}(p_{g_1}; r_{g_1}) \epsilon_{\mu_{g_2}}(p_{g_2}; r_{g_2}) \\ &\times \left\{ \eta^{\mu_{t_1} \mu_{t_3}} \left(t_1 \left(\frac{2p_{q_1}^{\mu_{g_1}}}{s_{q_1 g_1}} \right) \left(\frac{2p_{q_1}^{\mu_{g_2}}}{(s_{q_1 g_1} + s_{q_1 g_2})} \right) + t_3 \left(\frac{2p_{q_2}^{\mu_{g_2}}}{s_{q_2 g_2}} \right) \left(\frac{2p_{q_2}^{\mu_{g_1}}}{(s_{q_2 g_1} + s_{q_2 g_2})} \right) \right. \right. \\ &\quad \left. \left. - \frac{t_1 t_3}{t_2} \left(\frac{2p_{q_1}^{\mu_{g_1}}}{s_{q_1 g_1}} \right) \left(\frac{2p_{q_2}^{\mu_{g_2}}}{s_{q_2 g_2}} \right) \right) \right. \\ &+ \frac{1}{t_2} \tilde{v}_{3g}^{\mu_{t_1} \mu_{t_2} \mu_{g_1}}(-p_{t_1}, p_{t_2}, p_{g_1}) \tilde{v}_{3g}^{\mu_{t_2} \mu_{t_3} \mu_{g_2}}(-p_{t_2}, p_{t_3}, p_{g_2}) \\ &- \frac{t_1}{t_2} \left(\frac{2p_{q_1}^{\mu_{g_1}}}{s_{q_1 g_1}} \right) \tilde{v}_{3g}^{\mu_{t_1} \mu_{t_3} \mu_{g_2}}(-p_{t_2}, p_{t_3}, p_{g_2}) + \frac{t_3}{t_2} \tilde{v}_{3g}^{\mu_{t_1} \mu_{t_3} \mu_{g_1}}(-p_{t_1}, p_{t_2}, p_{g_1}) \left(\frac{2p_{q_2}^{\mu_{g_2}}}{s_{q_2 g_2}} \right) \\ &+ \frac{1}{s_{g_1 g_2}} \tilde{v}_{3g}^{\mu_{\sigma} \mu_{g_2} \mu_{g_1}}(-p_{g_1} - p_{g_2}, p_{g_2}, p_{g_1}) \left(v_{3g}^{\mu_{t_1} \mu_{t_2} \mu_{\sigma}}(-p_{t_1}, p_{t_3}, p_{g_1} + p_{g_2}) \right. \\ &\quad \left. - \frac{2q_1^{\mu_{\sigma}}}{(s_{q_1 g_1} + s_{q_1 g_2})} + \frac{2\bar{q}_2^{\mu_{\sigma}}}{(s_{q_2 g_1} + s_{q_2 g_2})} \right) \\ &\left. + 2\eta^{\mu_{t_1} \mu_{g_2}} \eta^{\mu_{t_3} \mu_{g_1}} - \eta^{\mu_{t_1} \mu_{t_3}} \eta^{\mu_{g_1} \mu_{g_2}} - 2\eta^{\mu_{t_1} \mu_{g_1}} \eta^{\mu_{t_3} \mu_{g_2}} \right\}. \end{aligned}$$

$$\begin{aligned} V_{g^* g g^* g}^{\mu_{t_1} \mu_{t_3}}(-p_{t_1}, p_{g_1}, p_{t_2}, p_{g_2}) &= i g_s \epsilon_{\mu_{g_1}}(p_{g_1}; r_{g_1}) \epsilon_{\mu_{g_2}}(p_{g_2}; r_{g_2}) \\ &\times \left\{ -\frac{1}{t_2} \tilde{v}_{3g}^{\mu_{t_1} \mu_{t_2} \mu_{g_1}}(-p_{t_1}, p_{t_2}, p_{g_1}) \tilde{v}_{3g}^{\mu_{t_2} \mu_{t_3} \mu_{g_2}}(-p_{t_2}, p_{t_3}, p_{g_2}) \right. \\ &- \frac{1}{t_2'} \tilde{v}_{3g}^{\mu_{t_1} \mu_{t_2}' \mu_{g_2}}(-p_{t_1}, p_{t_2}', p_{g_2}) \tilde{v}_{3g}^{\mu_{t_2}' \mu_{t_3} \mu_{g_1}}(-p_{t_2}', p_{t_3}, p_{g_1}) \\ &+ \frac{t_1}{t_2} \left(\frac{2p_{q_1}^{\mu_{g_1}}}{s_{q_1 g_1}} \right) \tilde{v}_{3g}^{\mu_{t_1} \mu_{t_3} \mu_{g_2}}(-p_{t_2}, p_{t_3}, p_{g_2}) - \frac{t_3}{t_2'} \left(\frac{2p_{q_2}^{\mu_{g_1}}}{s_{q_2 g_1}} \right) \tilde{v}_{3g}^{\mu_{t_1} \mu_{t_3} \mu_{g_2}}(-p_{t_1}, p_{t_2}', p_{g_2}) \\ &+ \frac{t_1}{t_2'} \left(\frac{2p_{q_1}^{\mu_{g_2}}}{s_{q_1 g_2}} \right) \tilde{v}_{3g}^{\mu_{t_1} \mu_{t_3} \mu_{g_1}}(-p_{t_2}', p_{t_3}, p_{g_1}) - \frac{t_3}{t_2} \left(\frac{2p_{q_2}^{\mu_{g_2}}}{s_{q_2 g_2}} \right) \tilde{v}_{3g}^{\mu_{t_1} \mu_{t_3} \mu_{g_1}}(-p_{t_1}, p_{t_2}, p_{g_1}) \\ &- \eta^{\mu_{t_1} \mu_{t_3}} \left(t_1 \left(\frac{2p_{q_1}^{\mu_{g_1}}}{s_{q_1 g_1}} \right) \left(\frac{2p_{q_1}^{\mu_{g_2}}}{s_{q_1 g_2}} \right) + t_3 \left(\frac{2p_{q_2}^{\mu_{g_1}}}{s_{q_2 g_1}} \right) \left(\frac{2p_{q_2}^{\mu_{g_2}}}{s_{q_2 g_2}} \right) - 2\eta^{\mu_{g_1} \mu_{g_2}} \right) \\ &\left. + t_1 t_3 \eta^{\mu_{t_1} \mu_{t_3}} \left(\frac{1}{t_2} \left(\frac{2p_{q_1}^{\mu_{g_1}}}{s_{q_1 g_1}} \right) \left(\frac{2p_{q_2}^{\mu_{g_2}}}{s_{q_2 g_2}} \right) + \frac{1}{t_2'} \left(\frac{2p_{q_2}^{\mu_{g_1}}}{s_{q_2 g_1}} \right) \left(\frac{2p_{q_1}^{\mu_{g_2}}}{s_{q_1 g_2}} \right) \right) \right\}. \end{aligned}$$

This looks complex, but the matrix-element evaluations are not computationally expensive.

NUMERICAL TEST OF $g^* ggg^*$ VERTEX: AMPLITUDE

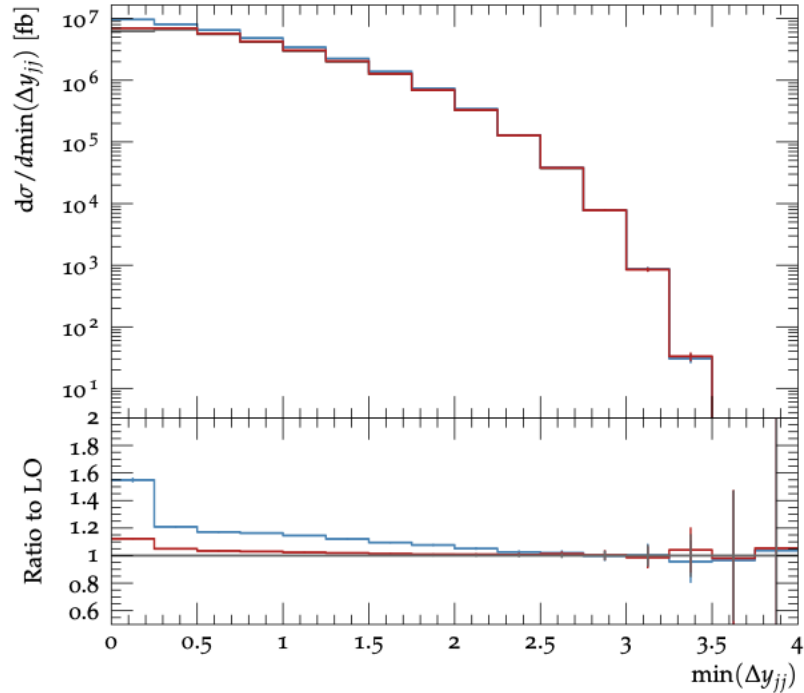
Here we compare the new HEJ $\mathcal{V}_{g^* ggg^*}^{\mu t_1 \mu t_3}$ vertex with the previous factorised approximations.



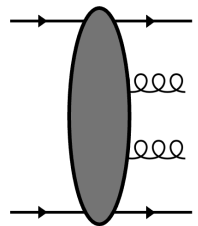
We see that the MRK approximation fails to describe the NMRK phase space. The strict approximation only begins to converge to LO at the edge of LHC phase space.

NUMERICAL TEST OF $g^* ggg^*$ VERTEX: CROSS SECTION

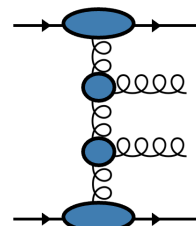
How well do the factorised expressions describe LO cross sections, within LHC phase space?



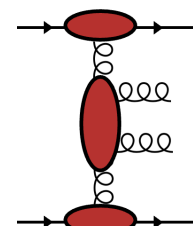
In these plots we compare the following factorised approximations to the exact LO amplitude:



$$\mathcal{M}_{qq \rightarrow qggg}$$



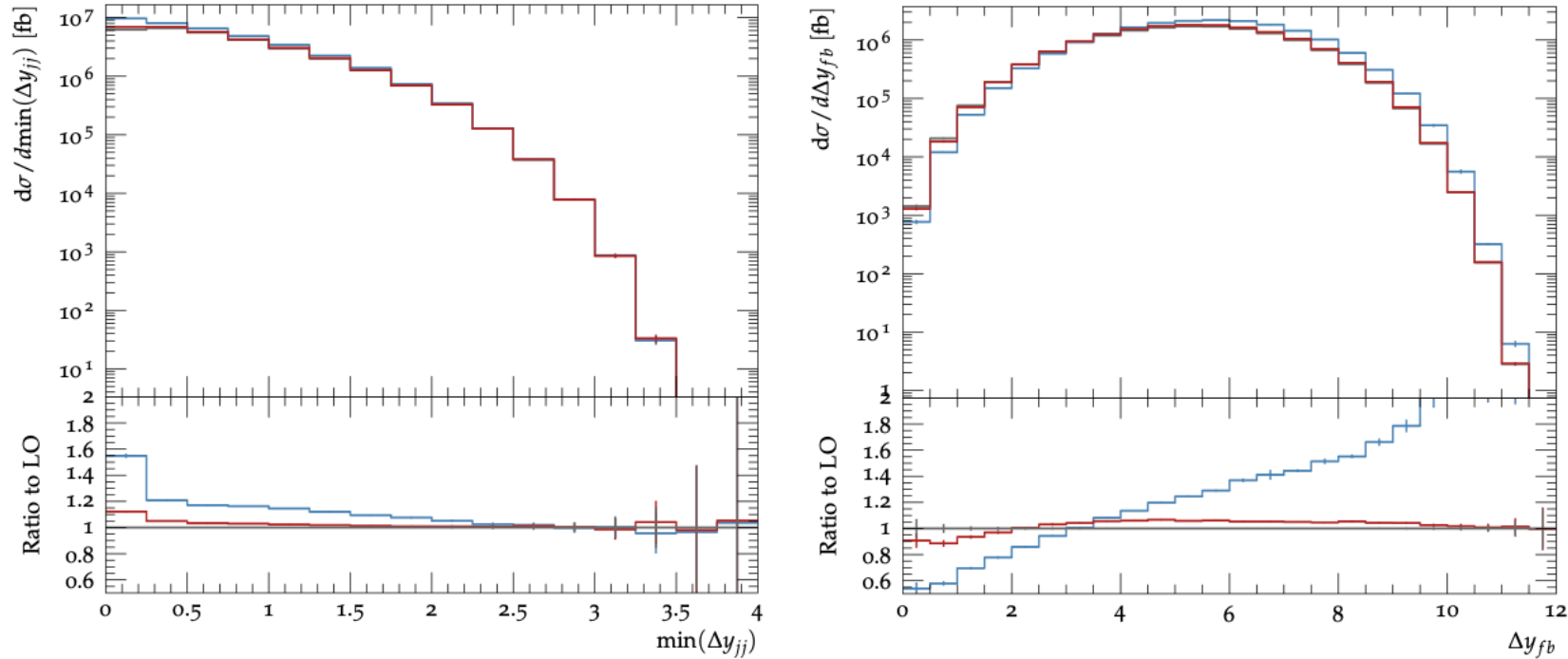
$$C_{q \rightarrow q} \frac{1}{t_1} \mathcal{V}_g \frac{1}{t_2} \mathcal{V}_g \frac{1}{t_3} C_{Q \rightarrow Q}$$



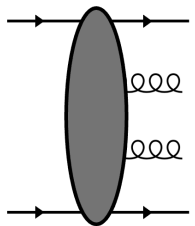
$$C_{q \rightarrow q} \frac{1}{t_1} \mathcal{V}_{gg} \frac{1}{t_3} C_{Q \rightarrow Q}$$

NUMERICAL TEST OF $g^* ggg^*$ VERTEX: CROSS SECTION

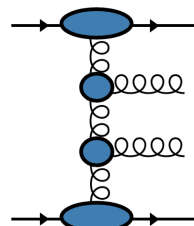
How well do the factorised expressions describe LO cross sections, within LHC phase space?



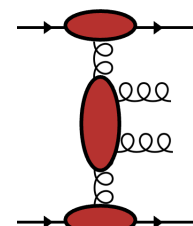
In these plots we compare the following factorised approximations to the exact LO amplitude:



$$\mathcal{M}_{qq \rightarrow qggq}$$



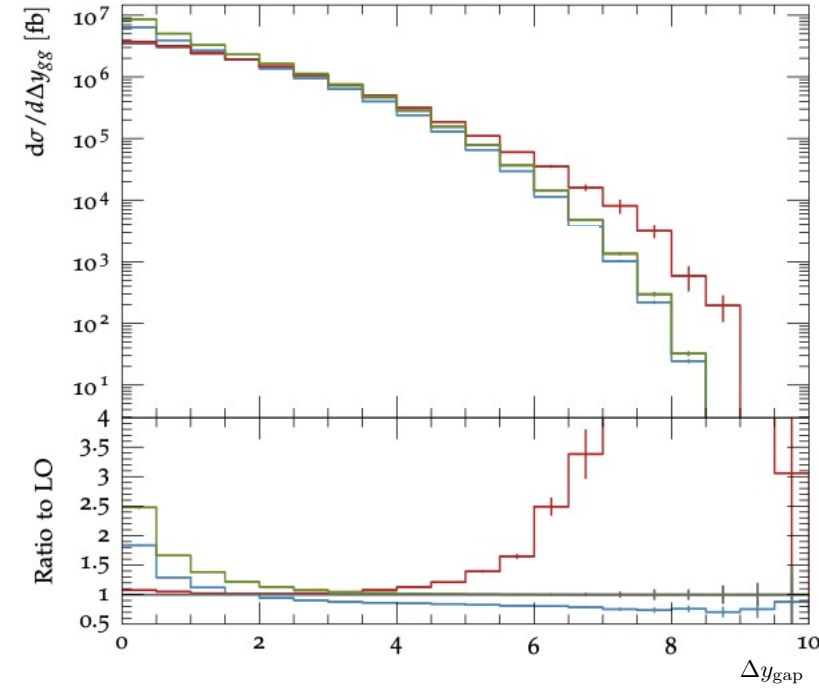
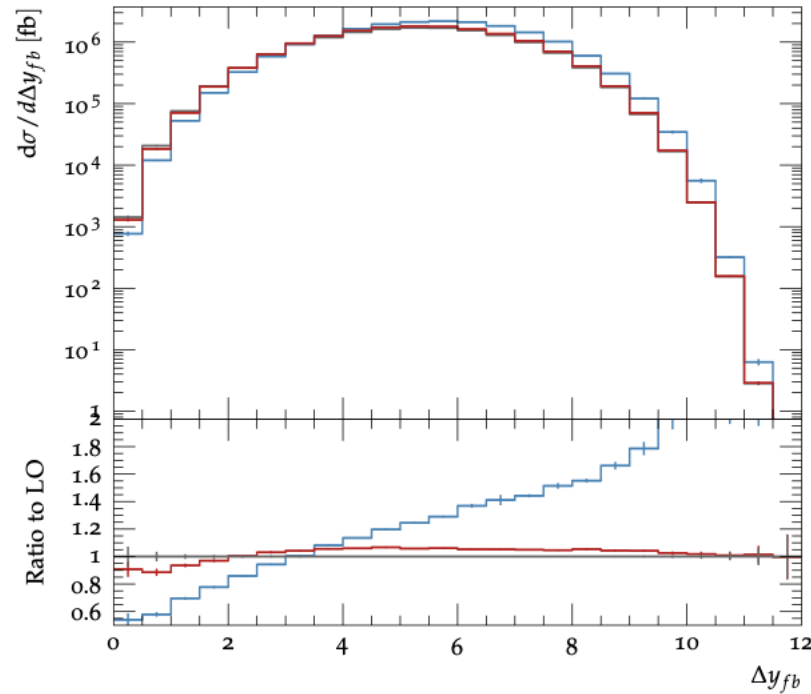
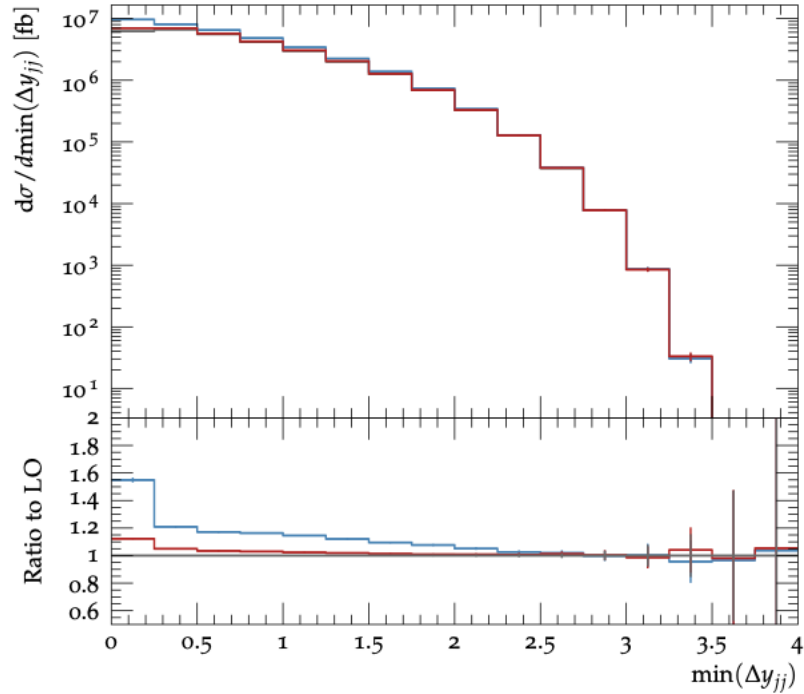
$$C_{q \rightarrow q} \frac{1}{t_1} \mathcal{V}_g \frac{1}{t_2} \mathcal{V}_g \frac{1}{t_3} C_{Q \rightarrow Q}$$



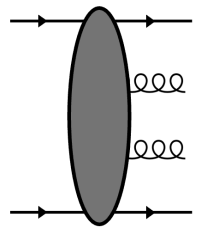
$$C_{q \rightarrow q} \frac{1}{t_1} \mathcal{V}_{gg} \frac{1}{t_3} C_{Q \rightarrow Q}$$

NUMERICAL TEST OF g^*ggg^* VERTEX: CROSS SECTION

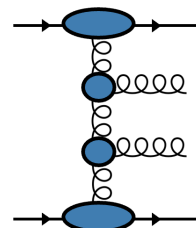
How well do the factorised expressions describe LO cross sections, within LHC phase space?



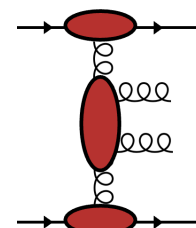
In these plots we compare the following factorised approximations to the exact LO amplitude:



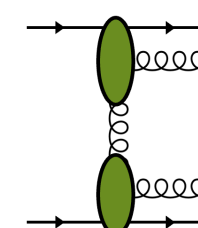
$$\mathcal{M}_{qq \rightarrow qggq}$$



$$C_{q \rightarrow q} \frac{1}{t_1} \mathcal{V}_g \frac{1}{t_2} \mathcal{V}_g \frac{1}{t_3} C_{Q \rightarrow Q}$$



$$C_{q \rightarrow q} \frac{1}{t_1} \mathcal{V}_{gg} \frac{1}{t_3} C_{Q \rightarrow Q}$$



$$C_{q \rightarrow qg} \frac{1}{t_2} C_{Q \rightarrow gQ}$$

CONCLUSIONS

In this talk we have introduced the main principles of the HEJ framework, and compared it with the BFKL approach.

We reviewed several advantages of adopting Monte Carlo for phase space integration. We focused on the freedom to take more complicated functions as our factorised building blocks.

This leads to improved descriptions away from the high-energy limit, while still capturing some of the high-energy physics.

ONGOING PROJECTS IN HEJ

As of the latest release, HEJ supports the following processes:

	Process	LL	Extremal g	Central qq
	≥ 2 jets	✓	✓	✓
[2210.10671]	H + \geq jet	✓	n/a	n/a
	H + ≥ 2 jets	✓	✓	
	W + ≥ 2 jet	✓	✓	✓
	Z/ γ + ≥ 2 jet	✓	✓	
[2107.06818]	W $^{\pm}$ W $^{\pm}$ + ≥ 2 jet	✓		

Current ongoing projects include:

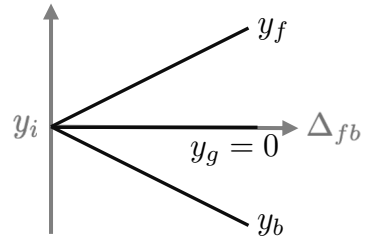
- Merging with Pythia
- Full NLL accuracy

The background is a vibrant, abstract composition of various geometric shapes and patterns. It includes a large light blue L-shaped block in the top left, a yellow circle partially overlapping a larger light blue circle with a white center in the top center, and a teal L-shaped block in the top right. A purple triangle with a white center is positioned in the lower middle. Other elements include a teal circle with a white center on the left, a black square with a white center on the right, and several black and white striped patterns. The overall style is modern and colorful.

Backup Slides

PHASE SPACE SLICES

3j MRK



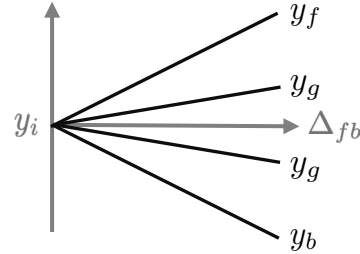
$$|p_{1\perp}| = |p_{2\perp}| = 40 \text{ GeV}$$

$$y_1 = \Delta, \quad y_2 = 0, \quad y_3 = -\Delta,$$

$$\phi_1 = 0, \quad \phi_2 = \frac{2\pi}{3},$$

$$p_{3\perp} = -p_{1\perp} - p_{2\perp}$$

4j MRK



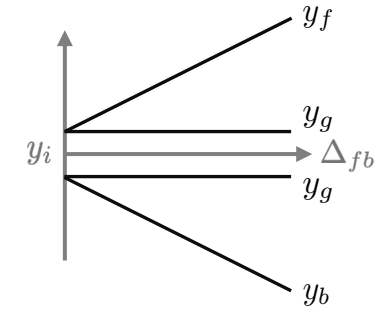
$$|p_{1\perp}| = |p_{2\perp}| = |p_{3\perp}| = 40 \text{ GeV}$$

$$y_1 = \frac{3\Delta}{2}, \quad y_2 = \frac{\Delta}{2}, \quad y_3 = -\frac{\Delta}{2}, \quad y_4 = -\frac{3\Delta}{2}$$

$$\phi_1 = 0, \quad \phi_2 = \frac{\pi}{4}, \quad \phi_3 = -\frac{3\pi}{2},$$

$$p_{4\perp} = -p_{1\perp} - p_{2\perp} - p_{3\perp}$$

4j NMRK



$$|p_{1\perp}| = |p_{2\perp}| = |p_{3\perp}| = 40 \text{ GeV}$$

$$y_1 = \Delta, \quad y_2 = 0.25, \quad y_3 = -0.25, \quad y_4 = -\Delta$$

$$\phi_1 = 0, \quad \phi_2 = \frac{\pi}{4}, \quad \phi_3 = -\frac{3\pi}{2},$$

$$p_{4\perp} = -p_{1\perp} - p_{2\perp} - p_{3\perp}$$